AIP Journal of Applied Physics

Electric-field-induced orthorhombic to monoclinic M B phase transition in [111] electric field cooled Pb (Mg 1/3 Nb 2/3 O 3) – 30 % Pb Ti O 3 crystals

Hu Cao, Jie-fang Li, and D. Viehland

Citation: Journal of Applied Physics **100**, 084102 (2006); doi: 10.1063/1.2359137
View online: http://dx.doi.org/10.1063/1.2359137
View Table of Contents: http://scitation.aip.org/content/aip/journal/jap/100/8?ver=pdfcov
Published by the AIP Publishing

Electric-field-induced orthorhombic to monoclinic M_B phase transition in [111] electric field cooled $Pb(Mg_{1/3}Nb_{2/3}O_3)-30\%PbTiO_3$ crystals

Hu Cao,[a] Jie-fang Li, and D. Viehland
Department of Materials Science and Engineering, Virginia Tech, Blacksburg, Virginia 24061

(Received 2 May 2006; accepted 25 July 2006; published online 18 October 2006)

Structural phase transformations of [111] electric field cooled (FC) $Pb(Mg_{1/3}Nb_{2/3})O_3-0.30PbTiO_3$ crystals have been performed by x-ray diffraction. A phase sequence of cubic $(C)\rightarrow$tetragonal $(T)\rightarrow$orthorhombic $(O)\rightarrow$monoclinic (M) was found in the FC condition. The finding of $a=b>c$ demonstrates that the M phase is of the M_B type. © *2006 American Institute of Physics*. [DOI: 10.1063/1.2359137]

I. INTRODUCTION

Solid solutions of $(1-x)Pb(Mg_{1/3}Nb_{2/3}O_3)-xPbTiO_3$ (PMN–xPT) and $(1-x)Pb(Zn_{1/3}Nb_{2/3}O_3)-xPbTiO_3$ (PZN–xPT) have a morphotropic phase boundary (MPB) between rhombohedral (R) and tetragonal (T) ferroelectric phases in the compositional ranges of $0.30<x<0.37$ (Ref. 1) and $0.08<x<0.11$,[2] respectively. High-resolution diffraction studies[1–7] have revealed additional "bridging" phases at the MPB that are of lower monoclinic (M) symmetry, initially reported in $Pb(Zr_{1-x}Ti_x)O_3$ ceramics[8–10] and subsequently in PZN–xPT (Refs. 2, 6, 7, and 11) and PMN–xPT (Refs. 1, 3–5, and 12) crystals. Monoclinic symmetry allows the polarization vector to be unconstrained within a plane rather than be constricted to a particular crystallographic axis as for the higher symmetry R, T, or orthorhombic (O) phases. Different polarization rotation paths have been observed, resulting in two types of monoclinic distortions M_A/M_B and M_C with space groups Cm and Pm, respectively, as illustrated in Fig. 1. The M_A/M_B unit cell has a unique b_m axis along the [110] direction and is doubled and rotated 45° about the c axis with respect to the pseudocubic cell; whereas the M_C unit cell is primitive, having a unique b_m axis that is oriented along the pseudocubic [010]. Both the M_A and M_B phases belong to the Cm space group; the difference lies in the magnitudes of the components of the polarization[13] corresponding to the pseudocubic cell: for M_A, $P_x=P_y<P_z$; whereas for M_B, $P_x=P_y>P_z$.

Room temperature x-ray studies by Noheda *et al.*[6] of PZN–8%PT have shown a phase sequence of $R\rightarrow M_A\rightarrow M_C\rightarrow T$ with increasing E beginning from the zero-field-cooled (ZFC) condition. When the field was removed, an O phase was observed to be stable, which can be viewed as a limiting M_C phase [$a_o=2a_m\sin(\beta/2)$; $b_o=2a_m\cos(\beta/2)$; $c_o=b_m$]. Similarly, neutron and x-ray studies of PMN–0.30PT (Ref. 3) with $E\|[001]$ have shown a $R\rightarrow M_A\rightarrow M_C\rightarrow T$ sequence with increasing E beginning from the ZFC; in addition, a $C\rightarrow T\rightarrow M_C\rightarrow M_A$ sequence was reported in the field-cooled (FC) condition. More recently, structural studies of [110] oriented PMN–30%PT crystals have shown a $C\rightarrow T\rightarrow O\rightarrow M_B$ phase sequence in the FC condition and a $R\rightarrow M_B\rightarrow O$ one at 300 K with increasing E beginning from the ZFC.[4] These results clearly show that the phase stability of PMN–xPT crystals is quite fragile—depending not only on electric field history, but also on crystallographic orientations along which E is applied. Furthermore, recent ε-E investigations of [111] oriented PZN–8%PT have revealed an induced phase transition, which is presumed to follow an $O\rightarrow M_B\rightarrow R$ phase sequence;[14] however, structural investigations were not reported with $E\|[111]$

In this present work, we establish the structural transformation sequence of PMN–30%PT crystals with $E\|[111]$ X-ray diffraction (XRD) studies with $E\|[111]$ unambiguously demonstrate a phase sequence of $C\rightarrow T\rightarrow O\rightarrow M_B$ for [111] FC PMN–30%PT, similar to that recently reported for $E\|[110]$ and distinctly different than the $C\rightarrow T\rightarrow M_C\rightarrow M_A$ for $E\|[001]$.

II. EXPERIMENT PROCEDURE

Single crystals of PMN–30%PT with dimensions of $3\times3\times3$ mm^3 were obtained from HC Materials (Urbana, IL) and were grown by a top-seeded modified Bridgman method. A cube sample was cut along $(111)/(1\bar{1}0)/(11\bar{2})$ planes, determined by an x-ray diffractometer with an error of ±0.5°.

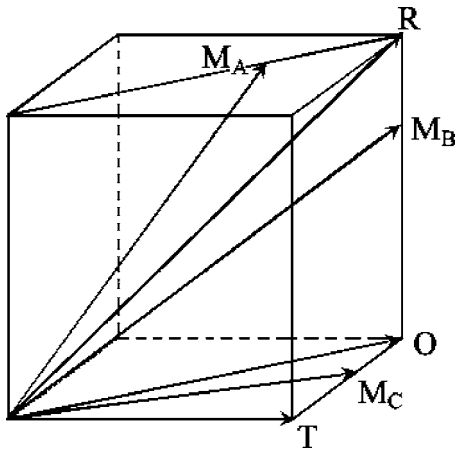

FIG. 1. Polarization vectors in the perovskite unit cell. The thick lines represent the rotation pathways followed by the end of the polarization vector in the monoclinic phases. The M_A, M_B, and M_C notations are adopted following Vanderbilt and Cohen (Ref. 13).

[a]Electronic mail: hcao@vt.edu

The crystal was finally polished using a 0.25 μm diamond polishing compound. Gold electrodes were deposited by sputtering. Temperature dependent dielectric constant measurements were performed using a multifrequency *LCR* meter (HP 4284A) under various E.

XRD studies were performed using a Philips MPD high-resolution system equipped with a two bounce hybrid monochromator, an open three-circle Eulerian cradle, and a doomed hot stage. A Ge (220)-cut crystal was used as an analyzer, which had an angular resolution of 0.0068°. The x-ray wavelength was that of Cu $K\alpha$=1.5406 Å, and the x-ray generator was operated at 45 kV and 40 mA. The penetration depth in the samples was on the order of 10 μm. For (111)-fielded PMN–0.30PT, the domain structure is quite complicated. In our studies, we obtained mesh scans about (i) the (002) reflection in the $(H\bar{H}L)$ zone defined by [001] and $[1\bar{1}0]$ vectors, (ii) the (200) reflection in the $(H\bar{L}L)$ zone defined by [100] and $[0\bar{1}1]$ vectors, and (iii) the (020) reflection in the $(HK\bar{H})$ zone defined by the [010] and $[10\bar{1}]$ vectors. We also obtained mesh scans about the (220), (022), and (202) reflections in each of their zones defined by [110] and $[1\bar{1}0]$, [011] and $[0\bar{1}1]$, and [101] and $[10\bar{1}]$, respectively. Each measurement cycle was begun by heating up to 550 K to depole the crystal, and measurements were subsequently taken on cooling. In this study, we fixed the reciprocal lattice unit (or 1 rlu) to $a^*=2\pi/a=1.560$ Å^{-1}. All mesh scans shown in this study were plotted in reference to this reciprocal unit.

III. RESULTS

To obtain a comprehensive picture of the PMN–30%PT structure properties in the FC condition for $E\|[111]$ we obtained mesh scans around the (002), (200), and (020) reflections at 393, 353, and 323 K as E=2 kV/cm, as shown in Fig. 2. In this study, the lattice parameters a, b, and c are those corresponding to those of the primitive unit cell. Although not presented, we also obtained (220), (022), (202), and (111) mesh scans. Table I shows the lattice parameters extracted from these mesh scans. The following are remarks of the mesh scan results.

(a) At 450 K, the contour maps around (002), (200), and (020) scans exhibited one peak (data not shown here). Analysis revealed a single lattice parameter, thus the structure is cubic with a_C=4.022 Å.

(b) At 393 K [see Figs. 2(a)–2(c)], (200) and (002) scans each exhibited a single peak, with different extracted lattice parameters of a=4.018 Å and c=4.031 Å; whereas the (020) scan exhibited a peak splitting along the longitudinal direction (0H0) but tilted along the transverse direction (0HH), with two different lattice constants. Please note that these values are quite close to those of c_T and a_T previously reported for [001] and [110] FC PMN–30%PT.[3,4] These results evidence that the structure is tetragonal and that multiple domain configurations exist along (020).

(c) At 353 K [see Figs. 2(d)–2(f)], the (002) and (020) reflections each exhibited only a single peak; whereas the (200) reflection revealed a second weaker one. Lattice parameters extracted from these reflections showed two values: $a=b\approx$4.027 Å and $c\approx$4.014 Å. In addition, two lattice parameters, 5.698 and 5.685 Å, were extracted from the (220) and (022) reflections (see Table I), which are very close to those of a_O and b_O of [110] FC PMN–30%PT.[4] These results evidence that the structure is orthorhombic with a_O=5.698 Å, b_O=5.685 Å, and c_O=4.014 Å.

(d) At 323 K [see Figs. 2(g)–2(i)], all of the reflections revealed only a single peak. Analysis showed that $a=b\approx$4.023 Å and $c\approx$4.019 Å. The fact that $a=b\neq c$

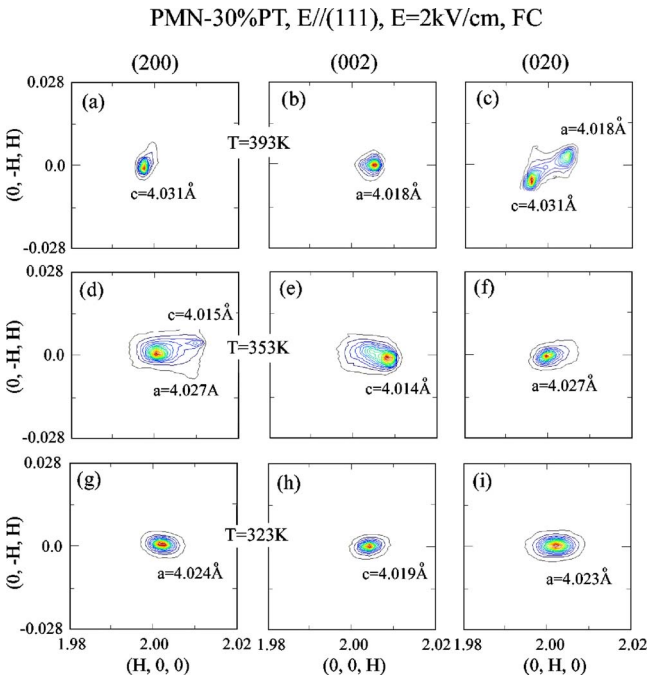

FIG. 2. (Color online) Mesh scans taken about the pseudocubic (200), (002), and (020) reflections for [111] electric field cooled PMN–0.30PT crystal with E=2 kV/cm at 393, 353, and 323 K.

TABLE I. Lattice parameters of the PMN–0.30PT, in the FC condition for $E\|(111)$, E=2 kV/cm.

	T=393 K (T)	T=353 K (O)	T=313 K (M_B)
(200)	c_T=4.031 Å	a=4.027 Å, c=4.015 Å	a=4.024 Å
(220)	⋯	a_o=5.699 Å, b_o=5.686 Å	a_{M_B}=5.695 Å, b_{M_B}=5.682 Å
(002)	a_T=4.018 Å	c=4.014 Å	c=4.019 Å
(022)	⋯	a_o=5.698 Å, b_o=5.685 Å	a_{M_B}=5.694 Å, a_{M_B}=5.682 Å
(020)	c_T=4.031 Å, a_T=4.018 Å	a=4.027 Å	a=4.023 Å
(202)	⋯	⋯	⋯

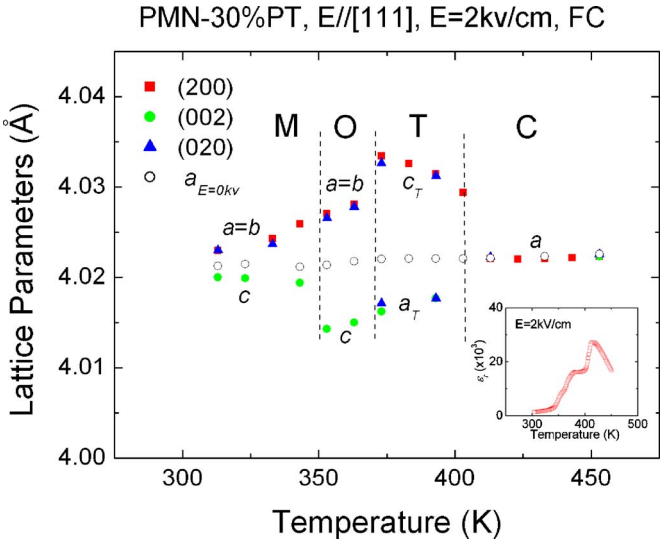

FIG. 3. (Color online) Lattice parameters as a function of temperature for a [111] electric field cooled PMN–0.30PT crystal with $E=2$ kV/cm. The inset gives the corresponding temperature dependence of the dielectric constant (1 kHz) with $E=2$ kV/cm, indicating a sequence of three phase transitions in the FC condition.

rules out the possibility of a R phase, although a field applied parallel to [111] might have been thought to favor it. The (220) and (022) reflections also revealed two different lattice parameters, 5.695 and 5.682 Å (see Table I). These values are quite close to those of a_{M_B}, b_{M_B} and c_{M_B} previously reported for [110] FC PMN–30%PT.[4] In addition, the finding of equivalence around the (200) and (020) reflections indicates that the polarization is constrained to the (110) plane and $a=b>c$ confirms that the new phase is M_B ($a_{M_B}=5.695$ Å, $b_{M_B}=5.682$ Å, and $c_{M_B}=4.019$ Å) instead of M_A.

To clarify the electric field effects on the phase sequence, we also investigated the temperature dependence of the lattice parameters of PMN–30%PT, as shown in Fig. 3. For comparison, the ZFC lattice parameters were also given. Above 410 K, the (200), (002), and (020) lattice parameters were all similar, both for FC and ZFC states, showing that PMN–30%PT has cubic symmetry at higher temperatures. On field cooling, a splitting of the lattice parameters was observed and a transformational sequence of $C\rightarrow T\rightarrow O\rightarrow M$ was found. Abrupt changes in the lattice parameter were found at the $C\rightarrow T$ transition, $c_T>a_C>a_T$. Important changes were also found at the $T\rightarrow O$ and $O\rightarrow M$ transitions. In the O phase, we found (i) the a and b lattice parameters of the primitive unit cell to be equivalent, but different than c; and (ii) that a_T and c_O vary continuously at the $T\rightarrow O$ transition, as previously reported for [001] and [110] FC PMN–30%PT.[3,4] On further cooling to the $O\rightarrow M$ transition, the values of a and b continuously decreased, while c underwent an abrupt change at a transition point of 343 K. The finding of $a=b>c$ confirms the structure to be monoclinic M_B rather than M_A. Furthermore, with further decreasing temperature, the lattice parameter a/b decreases gradually, whereas c increases gradually. It is expected that lattice parameters of M_B phase tend to be those of rhombohedral phase at lower temperature. Similarly, the dielectric behavior with $E=2$ kV/cm applied along [111] also revealed a sequence of three phase transitions on field cooling, as shown in the inset of Fig. 3, which is consistent with the lattice parameter evolution.

The results in Fig. 3 demonstrate that PMN–30%PT has a phase sequence of $C\rightarrow T\rightarrow O\rightarrow M_B$ on field cooling with $E//[111]$. This sequence is similar to that recently reported for $E//[110]$; both are different than the $C\rightarrow T\rightarrow M_C\rightarrow M_A$ one previously established for $E//[001]$. Table II summarizes the lattice parameters of the various phases in the transformation sequences for [001], [110], and [111] field-cooled PMN–30%PT crystals, where only slight variations in lattice parameters can be seen between the phases of the different sequences. It should be noted that the O phase is the limiting case of the M_C one:[1] accordingly, the O lattice parameters of the [111] and [110] field-cooled sequences are nearly equal to those of the M_C phase in the [001] sequence, with the distinction that β was slightly smaller in the M_C phase (90.07°) than in the O or limiting M_C one (90.12°). The principal difference in the sequences for the various FC states was the relative stability of the M_A/M_B phases at lower temperatures.

Prior x-ray diffraction investigations had shown that PMN–30%PT has a R phase at low temperature after electric field poling along [111]. Furthermore, polarized light microscopy studies of PZN–8%PT Ref. 14 and PMN–33%PT Ref. 15 have evidenced R domains under $E//[111]$. However, our results reveal that PMN–30%PT has a M_B-type structure in the FC condition, with $a=b>c$. We also performed struc-

TABLE II. Lattice parameters of the various phases in the transformation sequences for [001], [110], and [111] field-cooled PMN–0.30PT crystals.

$E\|\|$	393 K	353 K	313 K
(001)[a]	$a_T=4.017$ Å, $c_T=4.033$ Å	$c_{M_C}=4.029$ Å, $a_{M_C}=4.025$ Å $b_{M_C}=4.012$ Å, $\beta=90.07°$	$a_{M_A}=5.692$ Å, $b_{M_A}=5.681$ Å $c_{M_A}=4.025$ Å, $\beta=89.96°$
(110)[a]	$a_T=4.016$ Å $c_T=4.031$ Å	$a_O=5.701$ Å, $b_O=5.688$ Å $c_O=4.012$ Å	$a_{M_A}=5.696$ Å, $b_{M_B}=5.682$ Å $c_{M_B}=4.019$ Å, $\beta=89.85°$
(111)[b]	$a_T=4.018$ Å $c_T=4.031$ Å	$a_O=5.698$ Å, $b_O=5.686$ Å $a=b=4.027$ Å, $c=4.014$ Å	$a_{M_B}=5.695$ Å, $b_{M_B}=5.682$ Å $a=b=4.023$ Å, $c=4.019$ Å

[a]$E=1$ kV/cm along [001] (Ref. 3) or along [110] (Ref. 4).
[b]$E=2$ kV/cm and a, b, and c are with respect to the pseudocubic primitive cell.

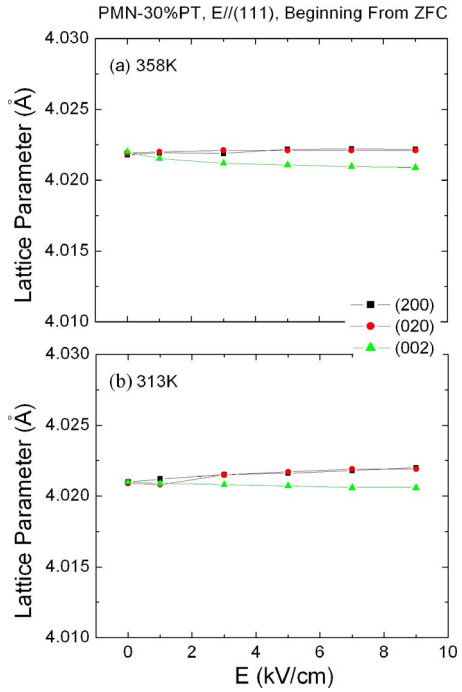

FIG. 4. (Color online) Electric field dependence of the lattice parameters for PMN–0.30PT with E//[111] beginning from the ZFC (R) phase taken at (a) 358 K, and (b) 313 K. These lattice parameters correspond to those of the primitive unit cell.

tural studies as functions of E with $E//[111]$, beginning with a previous ZFC condition, as shown in Fig. 4. This figure presents lattice parameters for PMN–30%PT as functions of field for $E//[111]$ taken at (a) 353 and (b) 313 K. In the ZFC condition, the (200), (020), and (002) lattice parameters were found to be equal; however, under $E//[111]$, the (002) lattice parameter can be seen to be less than the (200) and (020), which were equivalent. With increasing E, the difference between a/b and c then gradually increased.

Application of $E//[111]$ should not uniquely fix any particular {002} direction—as the (200), (002), and (200) reflections are threefold symmetric about [111]. However, as we have experimentally shown above in the mesh scans of Fig. 2, the (002) reflection is preferred. This has important consequences upon the transformational sequence for the [111] FC state: the [001] axis is the short axis all the way through the transformation, which was also observed in the [110] electric field cooled PMN–30%PT crystal.[4] The O phase, observed as a single domainlike state, bridges the T and M_B phases. We can understand the M_B phase by decomposing $E//[111]$ into its three constituent components ($E_{[100]}$, $E_{[010]}$, and $E_{[001]}$). In this case, the two components $E_{[100]}$ and $E_{[010]}$ are equivalent to $E//[111]$, where a single domain O phase would be favored;[4] then, the third component $E_{[001]}$ provides a degree of freedom for the polarization rotation of this single domain state along the $O \rightarrow R$ pathway, fulfilling the requirements for the M_B phase, as illustrated in Fig. 1.

It is an experimental observation that the O phase is a single domain state rather than one that decomposes into a polydomain one. It is likely that redistribution of strain inside of the crystal under $E//[111]$ plays an important role in the anisotropy of the crystal lattice, favoring a single domain macroscopic O and/or M_B phase. An interesting and plausible interpretation of this ferroelectric O or limiting M_C phase can be found in recent publications,[16–18] the so-called *adaptive phase*, based on the assumption of very small domain-wall energy. The adaptive state is inhomogeneous in the nanoscale, but appears homogeneous in the macroscale due to symmetry averaging: the nanoscale microstructure of this adaptive state is a miniaturized microdomain structure determined by the accommodation of the misfit-generated stress and electric field. In order to accommodate the stress and avoid misfits along the domain boundaries, certain relationships between the lattice parameters of the tetragonal phase (a_T, c_T) and the adaptive one (a_{ad}, b_{ad}, c_{ad}) need to be fulfilled—particularly, $a_{ad}+c_{ad}=a_T+c_T$ and $b_{ad}=a_T$—which have been experimentally verified for PMN–xPT and PZN–xPT.[17–19] Moreover, in the M_C phase, a relationship between the monoclinic angle (β) and the tetragonal/monoclinic lattice parameters has been obtained as $\beta=90°+2A\omega(1-\omega)\psi$,[19] where 2ψ is the angle formed by the two twin variants in the T phase, ω is the volume fraction of one of the variants, and A is a fitting parameter related to the volume fraction of domain walls. We note that the O structure is a limiting case of M_C, where $\omega=\frac{1}{2}$. We further note that this condition corresponds to tetragonal microdomains, whose a and c variants are equally populated.

In summary, structural phase transformation investigations of [111] FC PMN–30%PT crystal have been performed by x-ray diffraction. Comparison of the results for [001], [110], and [111] FC PMN–30%PT crystals reveals that PMN–30%PT with $E//[111]$ has a phase sequence of $C \rightarrow T \rightarrow O \rightarrow M_B$ on cooling. The discovery that $a=b>c$ under $E//[111]$ reveals that PMN–30%PT has features of a M_B-type structure.

ACKNOWLEDGMENTS

We would like to gratefully acknowledge financial support from the Office of Naval Research under Grant Nos. N000140210340, N000140210126, and MURI N0000140110761. We would like to thank H. C. Materias for providing the single crystals used in this study.

[1] B. Noheda, D. E. Cox, G. Shirane, J. Gao, and Z. G. Ye, Phys. Rev. B **66**, 054104 (2002).
[2] D. La-Orauttapong, B. Noheda, Z. G. Ye, P. M. Ghering, J. Toulouse, D. E. Cox, and G. Shirane, Phys. Rev. B **65**, 144101 (2002).
[3] F. Bai, N. Wang, J. Li, D. Viehland, P. Gehring, G. Xu, and G. Shirane, J. Appl. Phys. **96**, 1620 (2004).
[4] H. Cao, F. Bai, N. Wang, J. Li, D. Viehland, G. Xu, and G. Shirane, Phys. Rev. B **72**, 064104 (2002).
[5] H. Cao, F. Bai, J. Li, D. Viehland, G. Xu, H. Hiraka, and G. Shirane, J. Appl. Phys. **97**, 094101 (2004).
[6] B. Noheda, D. E. Cox, G. Shirane, S. E. Park, L. E. Cross, and Z. Zhong, Phys. Rev. Lett. **86**, 3891 (2001).
[7] K. Ohwada, K. Hirota, P. Rehrig, Y. Fujii, and G. Shirane, Phys. Rev. B **67**, 094111 (2003).
[8] B. Noheda, D. E. Cox, G. Shirane, J. A. Gonzalo, L. E. Cross, and S.-E. Park, Appl. Phys. Lett. **74**, 2059 (1999).
[9] B. Noheda, J. A. Gonzalo, L. E. Cross, R. Guo, S.-E. Park, D. E. Cox, and G. Shirane, Phys. Rev. B **61**, 8687 (2000).
[10] B. Noheda, D. E. Cox, G. Shirane, R. Guo, B. Jones, and L. E. Cross, Phys. Rev. B **63**, 014103 (2000).
[11] B. Noheda, Z. Zhong, D. E. Cox, G. Shirane, S. E. Park, and P. Rehrig, Phys. Rev. B **65**, 224101 (2002).

[12]Z. G. Ye, B. Noheda, M. Dong, D. Cox, and G. Shirane, Phys. Rev. B **64**, 184114 (2001).
[13]D. Vanderbilt and M. Cohen, Phys. Rev. B **63**, 094108 (2001).
[14]M. Davis, D. Damjanovic, and N. Setter, J. Appl. Phys. **97**, 064101 (2005).
[15]C.-S. Tu, V. H. Schmidt, I.-C. Shih, and R. Chien, Phys. Rev. B **67**, 020102 (2003).
[16]D. Viehland, J. Appl. Phys. **88**, 4794 (2000).
[17]Y. M. Jin, Y. U. Wang, A. G. Khachaturyan, J. F. Li, and D. Viehland, J. Appl. Phys. **94**, 1 (2003).
[18]Y. M. Jin, Y. U. Wang, and A. G. Khachaturyan, Phys. Rev. Lett. **91**, 197601 (2003).
[19]Y. Wang, Phys. Rev. B **73**, 014113 (2006).